Received: 24 May 2019 | Revised: 7 September 2019 | Accepted: 2 November 2019

DOI: 10.1002/joc.6394

RESEARCH ARTICLE

International Journal of Climatology RMetS

Changes in future rainfall extremes over Northeast Bangladesh: A Bayesian model averaging approach

Md. Abul Basher[1] | **A. K. M. Saiful Islam**[1] | **Mathew A. Stiller-Reeve**[2] | **Pao-Shin Chu**[3]

[1]Institute of Water and Flood Management (IWFM), Bangladesh University of Engineering and Technology (BUET), Dhaka, Bangladesh

[2]NORCE Norwegian Research Centre AS, Bergen, Norway

[3]Department of Atmospheric Sciences, School of Ocean and Earth Science and Technology, University of Hawaii-Manoa, Honolulu, Hawaii

Correspondence
A. K. M. Saiful Islam, PhD, Professor, Institute of Water and Flood Management (IWFM), Bangladesh University of Engineering and Technology (BUET), Dhaka 1000, Bangladesh.
Email: akmsaifulislam@iwfm.buet.ac.bd, saiful3@gmail.com

Funding information
FP7 Environment, Grant/Award Number: 603864; Research Council of Norway, Grant/Award Number: TRACKS

Abstract

In this paper, we used a Bayesian model averaging (BMA) approach to analyse the changes in rainfall extremes in the periods 2041–2070 and 2071–2099 over northeast Bangladesh as a consequence of climate change. Climate change over this region could potentially impact agricultural production, water resources management, and the overall economy of the country. We used six regional climate models (RCMs) over the Coordinated Regional Downscaling Experiment South Asia domain. We used one medium stabilization scenario (RCP4.5) and one high-emission scenario (RCP8.5) for projecting the extreme rainfall indices. A multi-model ensemble mean was generated using the BMA approach. The BMA mean is a weighted average related to each RCM's predictive skill during the training period. Most of the rainfall extremes are expected to increase in both pre-monsoon (March–May) and monsoon (June–September) seasons in the future compared with baseline (1976–2005). The average pre-monsoon rainfall of the study area is projected to increase by 12.93 and 18.42% under RCP4.5 and 18.18 and 23.85% under RCP8.5 for the periods 2041–2070 and 2071–2099, respectively. The average monsoon rainfall of the study area is projected to increase by 4.96 and 2.27% under RCP4.5 and 6.56 and 6.40% under RCP8.5 for the periods 2041–2070 and 2071–2099, respectively. All the extreme indices except consecutive wet day are expected to change significantly at the 95% confidence level during the pre-monsoon season. The study area will potentially be subjected to more frequent floods in the future both in pre-monsoon and monsoon seasons as a consequence of climate change. Notably, the intensity and the magnitude of flash flooding in the pre-monsoon season are expected to increase more in the future because the increase in extreme indices is more significant during that season.

KEYWORDS

Bayesian model averaging, climate change, multi-model ensemble mean, rainfall extremes, regional climate models, representative concentration pathways

1 | INTRODUCTION

Rainfall is a significant concern for northeast Bangladesh (Bremer, 2017). Heavy rain in the adjacent mountainous region of India causes flash flooding during the pre-monsoon season and prolongs riverine flooding during the monsoon season. Pre-monsoon flash floods can destroy the seasonal Boro rice harvest, which is the main

crop of the region (Alam *et al.*, 2010). Such events severely impact individual farmers, families, communities, and the region's food security. Therefore, it is essential to understand the past and future trend of the extreme rainfall events for future planning of water resources management. This paper uses new observational records, state-of-the-art climate simulations, and an advanced statistical method (namely Bayesian Model Averaging [BMA]) to describe possible changes in future rainfall extremes in northeast Bangladesh, during both the pre-monsoon and monsoon seasons.

Northeast Bangladesh (Figure 1) is located within the basin of the Meghna River. The total catchment area of the Meghna River is 6,500 km^2, of which roughly 33% lies in northeast Bangladesh and 67% lies in India (Masood and Takeuchi, 2016). The mountainous regions of the Indian states of Assam, Meghalaya, and Tripura are located upstream of the basin. The flat and low-lying areas of Bangladesh are located downstream of these regions. The mountains act as a barrier against the southwesterly moisture flow from the Bay of Bengal. Orographic lifting of moist air is one of the mechanisms that trigger rainfall in the region (Ohsawa *et al.*, 2001; Mahanta *et al.*, 2013; Sato, 2013; Stiller-Reeve *et al.*, 2015). The rainfall over

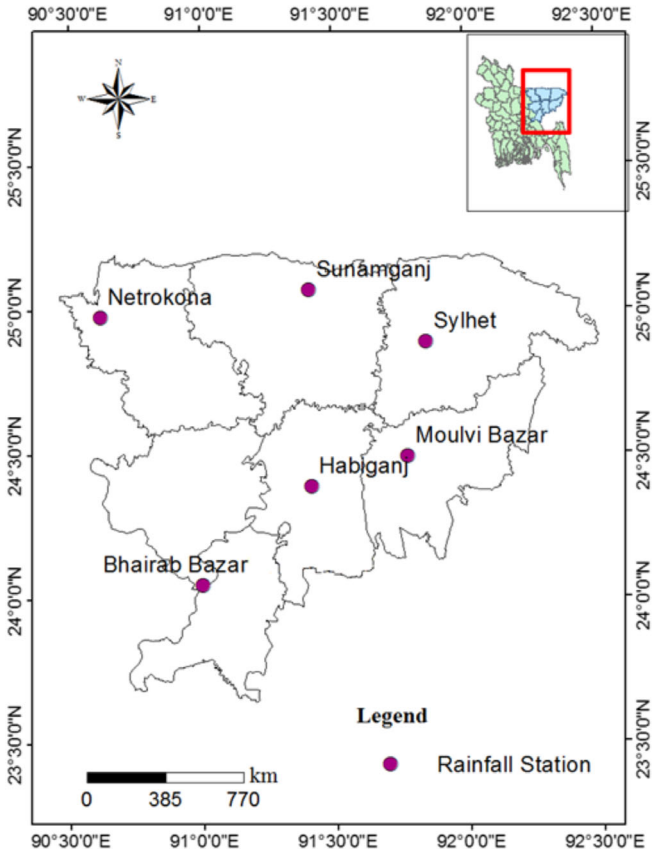

FIGURE 1 Study area with rainfall stations [Colour figure can be viewed at wileyonlinelibrary.com]

northeast Bangladesh and adjoining Indian hills can cause pre-monsoon flash floods and monsoon river floods in northeast Bangladesh. If rainfall changes in the future, how might that affect these events?

Kumar *et al.* (2006) and Revadekar *et al.* (2011)) studied the changes in seasonal rainfall and rainfall extremes, respectively, at the end of the 21st century over India and northeast Bangladesh. Nowreen *et al.* (2015) also studied the changes in rainfall extremes in the 21st century over northeast Bangladesh. These studies used an ensemble of simulations from a single RCM (developed by Hadley Centre of UK Meteorology Office) under emission scenarios (SRES A2, A1B, and B2) of IPCC AR4. The previous studies (Kumar *et al.*, 2006; Revadekar *et al.*, 2011; Nowreen *et al.*, 2015) found that one-day maximum rainfall, five-day maximum rainfall, and total rainfall during the pre-monsoon and monsoon seasons in northeast Bangladesh are projected to increase in the 21st century. Several other studies (Akhter *et al.*, 2017, Chen, 2013, Chen and Sun, 2013, Masood et al. 2015, Xu *et al.*, 2019, Wu and Huang, 2016) found that the extreme rainfall events over other parts of Asia are projected to significantly increase at the end of the 21st century.

To analyse future changes in rainfall extremes, we used the general circulation models (GCMs). GCMs simulate the present and future climate variability on global and continental scales under the different global warming scenarios or representative concentration pathways (RCPs). However, the coarse spatial resolution (100–300 km) of GCMs limits their application for impact studies at the regional scale (Zorita and Von Storch, 1999). Under the Coordinated Regional Climate Downscaling Experiment (CORDEX) of the World Climate Research Programme (WCRP), GCMs have downscaled with RCMs in a finer spatial resolution (10–50 km) under four different RCPs to assess the climate change impacts on human and natural systems at the regional to local scale (Giorgi *et al.*, 2009). The RCP scenarios evolve towards different radiative forcing at the end of the 21st century. For example, scenario RCP4.5 shows an increase in radiative forcing of 4.5 W m^{-2} by the end of the century relative to the pre-industrial conditions (Jacob *et al.*, 2014).

It is widely accepted that there are lots of uncertainty sources involved in climate change impact assessment. The primary sources of uncertainty in climate projections are the uncertainty in emission scenarios, model configuration, and model internal variability (Kay *et al.*, 2009; Wu *et al.*, 2015; Xu *et al.*, 2019). The uncertainty in emission scenarios can be examined by simulating different emission scenarios. The uncertainty in model configuration can be explored by using different model configurations (e.g., physics parameters) within the same modelling system. The uncertainty in model internal variability can be examined by executing different realizations of the same

scenario using different initial conditions (Giorgi *et al.*, 2009). These uncertainties in climate change projections need to be described fully to provide useful information for impact assessment studies. Where possible, these uncertainties may need to be reduced. Previous studies (e.g., Kumar *et al.*, 2006; Revadekar *et al.*, 2011; Nowreen *et al.*, 2015) on the study area were unable to describe the entire range of uncertainties because they used an ensemble of simulations from a single RCM (PRECIS-developed by Hadley Centre of UK Met Office). However, in this study, we used daily rainfall data from six RCMs over CORDEX South Asia domain (Table 1) under RCP4.5 as well as RCP8.5 to describe the entire uncertainty ranges as much as possible.

The downscaled rainfall data from the RCMs are affected by biases inherited from the forcing GCMs (Kato *et al.*, 2001). Even within a single geographic region, different RCMs may produce different results due to their model fundamentals and climate forcing (Rauscher *et al.*+, 2010; Déqué *et al.*, 2012; Mearns *et al.*, 2012; Zhang *et al.*, 2016). The biases in the RCMs include too much drizzle, errors in the mean, and failure to simulate heavy rainfall events (Piani *et al.*, 2010). Therefore, the output from RCMs needs to be corrected before applying for climate change impact studies (Maraun *et al.*, 2010; Teutschbein and Seibert, 2010; Winkler *et al.*, 2011). To correct the biases, we first need a set of observational data as ground truth. For this study, we used daily rainfall data from six rainfall stations of northeast Bangladesh (Table 2). Among these, five stations are maintained by the Bangladesh Water Development Board and one station is maintained by the Bangladesh Meteorological Department. Using these observations, we can reduce the biases in the RCM model data.

In recent years, several studies investigated different bias correction methods to provide a reliable estimator of observed precipitation climatology given RCM output (e.g., Chen *et al.*, 2011; Turco *et al.*, 2011; Teutschbein and Seibert, 2012; Themeßl *et al.*, 2012). The simplest method is the delta correction method in which an average bias (delta) for a specified period (Lehner *et al.*, 2007) is used to correct the bias. A linear transformation function between one or more predictors and the predictand is used in multiple linear regression method (e.g., Hay and Clark, 2003; Horton *et al.*, 2006). This method is used to adjust mean and variance only of the observed and the simulated rainfall. Alternatively, the local intensity scaling method can adjust the mean as well as both wet-day frequencies and wet-day intensities of precipitation time series (Schmidli and Frei, 2005). The power transformation method corrects the mean and variance of precipitation by applying a non-linear correction in an exponential form (Leander and Buishand, 2007; Leander *et al.*, 2008). In this method, the long-term monthly mean of the daily simulated precipitation series is mapped with the monthly mean of observed precipitations. Distribution mapping is a relatively modern approach in which the distribution of RCM

TABLE 1 List of RCMs and their driving models

RCM	Driving GCM	Experiment name	Institute
ACCESS	ACCESS1-0	ACCESS-CSIRO-CCAM	CSIRO
CCSM4	CCSM4	CCSM4-CSIRO-CCAM	CSIRO
CNRM	CNRM-CM5	CNRM-CM5-CSIRO-CCAM	CSIRO
MPI	MPI-ESM-LR	MPI-ESM-LR-CSIRO-CCAM	CSIRO
MPI- REMO	MPI-M-MPI-ESM-LR	MPI-CSC-REMO2009	MPI-CSC
SMHI	ICHEC, EC-EARTH	ICHEC-EC-EARTH-SMHI-RCA4	SMHI

TABLE 2 List of rainfall stations and their locations. The mean of the pre-monsoon and monsoon rainfall was calculated for the period of 1976–2005

Station name	District	Location of station (latitude, longitude)	Pre-monsoon mean rainfall (mm)	Monsoon mean rainfall (mm)
Sylhet	Sylhet	24.90°N, 91.88°E	1,087	2,733
Sunamganj	Sunamganj	25.06°N, 91.44°E	1,095	4,435
Netrokona	Netrokona	24.98°N, 90.62°E	670	2,485
Moulvibazar	Moulvibazar	24.49°N, 91.70°E	740	1890
Habiganj	Habiganj	24.39°N, 91.41°E	695	1,525
Bhairabbazar	Kishoreganj	24.05°N, 91.00°E	580	1,330

simulated climate data is matched with the distribution of the observed climate data to correct the distribution of the RCM simulated climate data. A transfer function is generated to shift the occurrence distributions of precipitation and temperature (Sennikovs and Bethers, 2009). Among the various methods, distribution mapping-based methods are getting more popular and have been applied to the downscale and correct temperature and precipitation data from RCMs in hydrological studies (Ashfaq *et al*., 2010; Piani *et al*., 2010; Dosio and Paruolo, 2011; Themeßl *et al*., 2012). Therefore, in this study, we used the quantile mapping bias correction method because it has been successfully and widely applied in climate change studies (Teutschbein and Seibert, 2010, 2012; Räisänen and Räty, 2013; Villani *et al*., 2015). In this method, cumulative distribution functions (CDFs) were first generated for both the observed and RCM-simulated rainfall. Thereafter, the CDF from an RCM simulated value is matched to the observed value at the same CDF over a specified base period (Kim *et al*., 2015). All the daily rainfall values from the RCMs are scaled up or down according to the adjusted CDF, which results in six corrected RCMs.

With the six corrected RCM simulations, we can take a multi-model ensemble mean to analyse possible future changes. Multi-model ensemble means have been shown to outperform individual model output also at the regional level (Pierce *et al*., 2009). Among several methods, the BMA method provides a more reasonable ensemble mean (Raftery *et al*., 2005; Vrugt and Robinson, 2007; Zhu *et al*., 2013) because it gives higher weight to the RCM with better predictive skill in the training period (Zhang *et al*., 2019). To the best of our knowledge, this is the first study on rainfall changes over northeast Bangladesh using RCMs under the CORDEX framework and the observational data set we have at our disposal.

This paper is divided into four sections. Section 2 covers a brief description of the data and methodology, including bias correction and multi-model ensemble mean method. Section 3 presents the discussion on results, which include BMA weights and future changes in rainfall extremes. Conclusions are presented in Section 4.

2 | DATA AND METHOD

2.1 | Study area

The study area is in northeast Bangladesh, which is located in the downstream part of the Meghna basin. It is characterized by a large number of extensive wetlands, which are locally called 'haors'. The haors are bowl-shaped, low-lying floodplains with unique characteristics—they are dry in the winter months and flooded during the monsoon season. The region is also characterized by several special topographical features, such as hills, hillocks, extensive protected forests, and large tea and rubber gardens. From a climatic perspective, the region is categorized by sub-tropical humid conditions (Hasan *et al*., 2012). The dry winter (December to February), pre-monsoon (March to May), monsoon (June to September), and post-monsoon (October to November) are the predominant seasons of this area (Islam and Uyeda, 2007; Rafiuddin *et al*., 2010). The haors are mostly dry during December to May, therefore Boro rice is extensively cultivated in during this time. The Boro rice harvest during the pre-monsoon accounts for the majority of agricultural output (Alam *et al*., 2010) and contributes significantly to the country's total rice production. Pre-monsoon rainfall is, therefore, a significant concern for this region.

Cherrapunji, one of the wettest places on Earth, is located upstream of the Meghna basin. The mountainous regions of the Indian states of Assam, Meghalaya, and Tripura act as a barrier against humid southwesterly flows from the Bay of Bengal. Orographic lifting and other mechanisms (Ohsawa *et al*., 2001; Mahanta *et al*., 2013; Sato, 2013; Stiller-Reeve *et al*., 2015) cause the heavy rainfall over the Meghna basin. This heavy rainfall during April and May causes flash floods in the flat and low-lying areas of Bangladesh and damages entire crops, as seen in April 2017. However, in this study, we only considered the downstream part of the basin due to the limitation of the observed data from the upstream part of the basin.

2.2 | Data

We used gridded daily rainfall data from six RCMs over CORDEX South Asia domain (Table 1) and observed daily rainfall data from six rainfall stations in northeast Bangladesh (Table 2) for this study. Here, we used the last 30 years (1976–2005) of the historical RCM runs and the corresponding observed daily rainfall from six weather stations in northeast Bangladesh. We used daily rainfall from RCMs for RCP4.5 as well as RCP8.5 for the period of 2041–2070 and 2071–2099 to project future rainfall extremes for the study area. The output of RCMs is available at the spatial resolution of 0.5°. The locations of weather stations do not match RCM grid points exactly. In this situation, we calculated RCM output at a weather station's location by interpolating (Inverse Distance Weighting method) four RCM grid points within which the station lies. Details of the RCMs and rainfall stations are presented in Tables 1 and 2, respectively.

2.3 | Methodology

In this study, we determined the changes in pre-monsoon and monsoon extremes rainfall indices (listed in Table 3)

TABLE 3 List of indices of rainfall extremes used for future projection and their definition

Index	Descriptive name	Definition	Unit
RX1	Daily maximum rainfall	Seasonal maximum 1-day rainfall	mm
RX5	5-day maximum rainfall	Seasonal maximum 5-day rainfall	mm
R25	Frequencies in days	Number of extremely heavy rainfall days (RR ≥25 mm) during pre-monsoon	days
R50	Frequencies in days	Number of extremely heavy rainfall days (RR ≥50 mm) during monsoon.	days
PRCPTOT	Seasonal total wet day precipitation	Seasonal total precipitation in wet days (RR ≥1 mm)	mm
CWD	Consecutive wet days	Maximum number of consecutive wet days in a season with RR ≥1 mm	days
CDD	Consecutive dry days	Maximum number of consecutive dry days in a season with RR < 1 mm	days
SDII	Simple daily intensity index	Seasonal total precipitation divided by the number of wet days in the season	mm/day
R95p	Very wet days	Seasonal total PRCP when RR > 95th percentile	mm
R99p	Extremely wet days	Seasonal total PRCP when RR > 99th percentile	mm

of northeast Bangladesh for 2041–2070 and 2071–2099 from six RCMs over the CORDEX South Asia region. We used 1976–2005 as a reference period and 2041–2070 and 2071–2099 as the two scenario periods in our analysis.

The RCMs often show a considerable systematic error that limits their application in impact studies. In climate change impact studies, the most common way to deal with this error is to apply bias correction on RCM outputs. In this study, we used the quantile mapping method to daily data on a seasonal basis. After correcting the biases, the multi-model ensemble mean of the extreme rainfall indices was generated by the BMA approach.

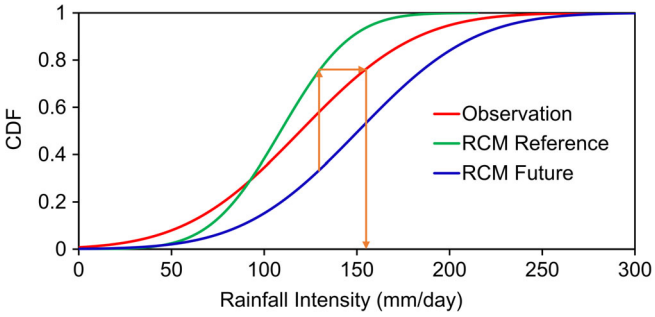

FIGURE 2 A schematic representation of quantile mapping bias-correction approach. A transfer function is used to correct rainfall intensity for RCM simulations during the reference and scenario period [Colour figure can be viewed at wileyonlinelibrary.com]

2.3.1 | Quantile mapping bias correction

Both the parametric and nonparametric quantile mapping method are widely used for bias correction of the climate model. However, the parametric method generally yields a better result (Kim *et al*., 2015) than the nonparametric method. This is because the parametric method can adjust the distributions of model output to agree with observed distributions. For this study, we chose gamma distribution method because it generally represents rainfall data well, particularly for monthly and seasonal values (Katz, 1999; Piani *et al*., 2010; Kim *et al*., 2015). We applied this method to both the reference and scenario periods. Generally, RCMs simulate too many rainfall events with low intensity compared with the observed rainfall, which is widely known as the drizzle effect (Kim *et al*., 2015). A brief procedure of the quantile mapping bias correction is as follows.

Step 1: In order to adjust the wet-day frequency of RCM-simulated rainfall according to observed rainfall, a cut-off threshold corresponding to the wet day (≥1 mm) is selected before applying quantile mapping method.

Step 2: The gamma CDF of the observed and RCM reference rainfall is determined for each month separately.

Step 3: The CDF of RCM reference simulation is mapped with CDF of observations for generating the transfer function. The schematic representation is presented in Figure 2.

Step 4: Then, this correction function is finally used to correct the RCM scenario period. The equation of the transfer function can be expressed as:

$$P^{*}_{\mathrm{ref}}(d)=F^{-1}_{\gamma}\left(F_{\gamma}\left(P_{\mathrm{ref}}(d)|\alpha_{\mathrm{ref},m},\beta_{\mathrm{ref},m}\right)|\alpha_{\mathrm{obs},m},\beta_{\mathrm{obs},m}\right) \quad (1)$$

$$P^{*}_{\mathrm{scen}}(d)=F^{-1}_{\gamma}\left(F_{\gamma}\left(P_{\mathrm{scen}}(d)|\alpha_{\mathrm{ref},m},\beta_{\mathrm{ref},m}\right)|\alpha_{\mathrm{obs},m},\beta_{\mathrm{obs},m}\right) \quad (2)$$

where $P_{\mathrm{ref}}(d)$ is the raw daily rainfall for reference simulation; $P_{\mathrm{scen}}(d)$ is the raw daily rainfall for scenario simulation; $P^{*}_{\mathrm{ref}}(d)$ is the bias-corrected daily rainfall for reference simulation; $P^{*}_{\mathrm{scen}}(d)$ is the bias-corrected daily rainfall for scenario simulation; F^{-1}_{γ} is the transfer

function for gamma distribution; $\alpha_{obs,\ m}$ is the shape parameter of gamma distribution for observed data of month m; $\alpha_{ref,\ m}$ is the shape parameter of gamma distribution for the reference period of month m; $\beta_{obs,\ m}$ is the scale parameter of gamma distribution for observed data of month m; $\beta_{ref,\ m}$ is the scale parameter of gamma distribution for the reference period of month m.

2.3.2 | Bayesian model averaging (BMA) Approach

BMA produces a complete PDF of the ensemble mean and quantifies the associated uncertainty of the forecasts. The BMA method has become increasingly popular because it produces accurate and reliable multi-model ensemble mean (Raftery *et al*., 1997; Neuman, 2003; Ajami *et al*., 2007). In this approach, the predictive probability density function (PDF) of the ensemble mean is the weighted average of the conditional PDF of an individual model. These weights are posterior probabilities of the models generating the forecasts and reflect the relative contributions of each model to the overall predictive skill. Hoeting *et al*. (1999) comprehensively described the BMA theory and Raftery *et al*. (2005) extended it for statistical post-processing of forecast ensembles. Given the training data Y^T and k climate models (M_1.... M_k), the forecast PDF of a variable Y is given by:

$$P(Y|Y_1,Y_2,.....Y_k)=\sum_{k=1}^{k}P(Y|M_k)P\left(M_k|Y^T\right) \quad (3)$$

where $P(Y|M_k)$ is the conditional PDF of Y on M_k, given that M_k is the best forecast in the ensemble and $P(M_k|Y^T)$ is the posterior probability of the model M_k being the best one given the training data. The posterior model probabilities reflect how the model M_k performs to fit the training data and can be viewed as weights that are non-negative and add up to one so that $\sum_{k=1}^{k}w_k=\sum_{k=1}^{k}P\left(M_k|Y^T\right)=1$. Thus, Equation (3) can be written as

$$P(Y|Y_1,Y_2,.....Y_k)=\sum_{k=1}^{k}w_kP(Y|M_k). \quad (4)$$

The BMA method assumes that the conditional PDF, $P(Y|M_k)$, of the individual model can be approximated by the normal distribution with mean $a_k + b_kM_k$ and standard deviation (SD) σ_k, which is given by.

$$P(Y|M_k)\sim N(a_k+b_kM_k,\sigma_k^2 \quad (5)$$

The values for a_k and b_k are estimated by simple linear regression of $P(Y|M_k)$ on M_k for each model. In this study, we determined BMA weight for all extreme rainfall indices (listed in Table 3) separately. At first, we derived the monthly values of extreme rainfall indices from a daily time series. Then, we separated the indices of pre-monsoon and monsoon seasons. By doing so, we have three values for the pre-monsoon and four values for the monsoon season for each index. In this way, for a 30-year period, we obtain a time series consisting of 90 values for the pre-monsoon season and 120 values for the monsoon season for the BMA computation. However, beforehand, we need to know the distribution of the indices according to the above discussions. For example, we fitted monthly rainfall totals of a particular season for different distributions (e.g., normal, gamma, and exponential) to determine which specific distribution data sample is best fitted. Using the Kolmogorov–Smirnov test and graphical techniques (histograms and density estimate), we found that the gamma distribution best fits the monthly rainfall data for the study area. As an example, a data histogram and the corresponding fitted gamma PDF for monthly rainfall of Sylhet station are shown in Figure 3. As expected, rainfall data are positively skewed with a long tail to the right of the distribution for both pre-monsoon and monsoon seasons. The gamma distribution, while being asymmetric and bounded on the left by zero, provides a good fit to the empirical data, particularly in the extreme left and right tails of the distribution.

Therefore, we considered the gamma distribution and modified the conditional PDF in Equation 5. The conditional PDF for the gamma distribution with shape parameter α and scale parameter β can be given by

$$P(Y|M_K)\sim\frac{1}{\beta\Gamma(\alpha)}Y^{\alpha-1}\exp\left(-Y/\beta\right) \quad (6)$$

for $Y > 0$. $P(Y|M_K) = 0$ for $Y \leq 0$. The mean of this distribution is $\mu = \alpha\beta$ and its variance is $\sigma^2 = \alpha\beta^2$. The parameters $\alpha_k=\mu_k^2/\sigma_k^2$ and $\beta_k=\sigma_k^2/\mu_k$ of the gamma distribution for the actual forecast Y_k of a particular ensemble member can be derived from the following relationship

$$\mu_k=Y_k \quad (7)$$

and

$$\sigma_k^2=c_0Y_k+c_1 \quad (8)$$

where c_0 and c_1 are the coefficients of regression.

Thus BMA multi-model ensemble mean is a conditional expectation, which is defined as

$$\bar{Y}=E\lceil Y|M_{1,}.....M_k\rceil. \quad (9)$$

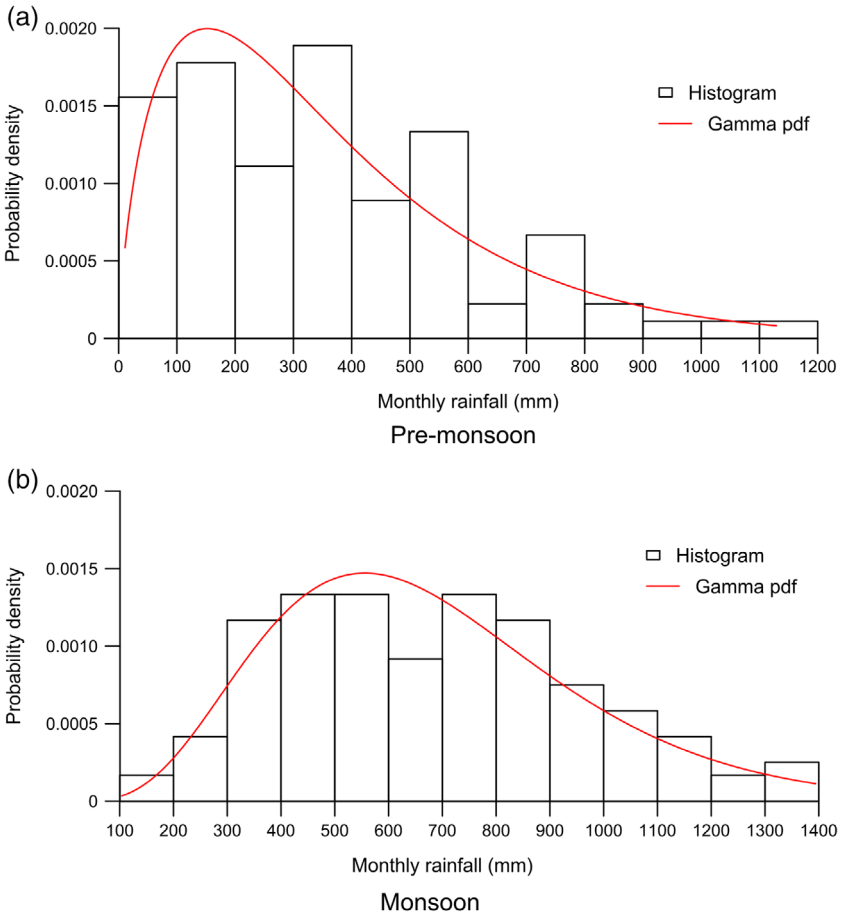

FIGURE 3 Histogram and gamma PDF for monthly rainfall of Sylhet station during (a) pre-monsoon and (b) monsoon [Colour figure can be viewed at wileyonlinelibrary.com]

The values of w_k, σ_k, c_0, and c_1 are estimated by the maximum likelihood (ML) function from simulated data set for the training period. The log-likelihood function $\mathcal{L}$ for the BMA multi-model ensemble mean in Equation (9) can be given as

$$\mathcal{L}\left(w_1,\ldots,w_k,\sigma^2|M_1,\ldots M_k, P(Y|M_K)\right) = \sum_{n=1}^{N}\log\left(\sum_{k=1}^{k} w_k P(Y_n|M_{kn})\right) \quad (10)$$

where N is the total number of measurements in the training dataset.

To derive the ML estimation of model parameters, a common approach is to use an expectation–maximization algorithm (Chu and Zhao, 2011; Chu *et al.*, 2016). Given an initial set of the model parameters, the expectation–maximization algorithm will converge quickly to a fixed set of parameter estimations after a few iterations. However, there are some inherent limitations of expectation–maximization: (a) it provides a local optimal solution instead of the global convergence and (b) it does not yield the uncertainty associated with final BMA weights and the variance (Vrugt *et al.*, 2008). To overcome this limitation, we optimize the ML function using the Differential Evolution Adaptive Metropolis (DREAM) Markov Chain Monte Carlo algorithm for estimating the BMA weights and variance (Vrugt *et al.*, 2008; Vrugt, 2015; Vrugt, 2016). The DREAM scheme is adapted from the Shuffled Complex Evolution Metropolis global optimization algorithm and is capable of running multiple chains simultaneously for searching the global optimal solution (Vrugt *et al.*, 2008).

3 | RESULTS AND DISCUSSIONS

3.1 | Quantile mapping bias correction

We performed the bias correction on daily rainfall data for the pre-monsoon and monsoon season independently after modifying wet-day frequencies of the RCM-simulated rainfall as discussed before. As an example, we use the results from the Sylhet station (Figure 4). The result of this bias correction for other stations is similar to the result shown in Figure 4 (see Figures S1 and S2).

Most of the uncorrected RCMs overestimate the high-intensity observed rainfall. However, it underestimates the low-intensity rainfall and produces too many drizzle

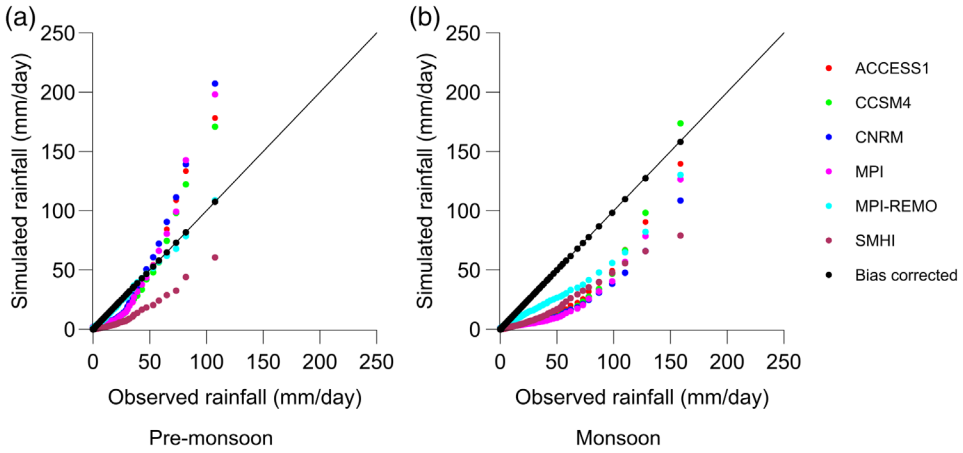

FIGURE 4 Quantile–quantile plots of simulated daily rainfall by RCMs against observed daily rainfall for Sylhet during (a) pre-monsoon and (b) monsoon. The colour markers denote uncorrected and black markers denote bias-corrected daily rainfall [Colour figure can be viewed at wileyonlinelibrary.com]

TABLE 4 Seasonal rainfall for Sylhet station before and after bias correction

		Observed	ACCESS	CCSM4	CNRM	MPI	MPI- REMO	SMHI
Pre-monsoon	Before bias correction	1,087	1,116	1,050	1,239	1,134	1,088	386
	After bias correction	1,087	1,090	1,072	1,079	1,081	1,059	1,076
Monsoon	Before bias correction	2,733	1,171	1,168	976	1,049	1,760	982
	After bias correction	2,733	2,707	2,700	2,710	2,719	2,712	2,712

days during the pre-monsoon season (Figure 4). Seasonal total rainfall of Sylhet station before and after bias correction is shown in Table 4 as an example. All RCMs simulate an almost equal amount of pre-monsoon rainfall except SMHI for Sylhet station. Note that the simulated seasonal rainfall from four (ACCESS, CCSM4, MPI, and MPI-REMO) of six RCMs is close to the observed amount (1,087 mm). After bias correction, the RCM simulation is closer to the actual seasonal rainfall, and this improvement is particularly evident for SMHI and CNRM RCMs. Among all six RCMs, the most substantial seasonal rainfall difference between simulation and observation is only 28 mm after bias correction.

During the monsoon season, all six RCMs underestimate the observed daily rainfall considerably from low to high intensity (Figure 4). As a result, all the RCMs underestimate the seasonal rainfall (Table 4). The RCM rainfall for Sylhet also showed similar behavior at other stations. However, after the bias correction, the RCM rainfall distributions and total amounts are similar to those of the observed rainfall. The most substantial seasonal rainfall difference between RCMs and the observation is only 33 mm.

A comparison of the variability (e.g., *SD*) between the bias-corrected and uncorrected simulations is presented in Figures 5 and 6. From the figures, we can see that the *SD* of the RCMs was not close to the *SD* of the observed rainfall before bias correction for both pre-monsoon and monsoon season. However, the *SD* of all RCMs was adjusted almost equal to the *SD* of the observed rainfall after bias correction.

3.2 | Bayesian model averaging

Although we calculated BMA weights for all extreme rainfall indices listed in Table 3, the results of the BMA weights for the pre-monsoon and monsoon rainfall are presented here as an example. Figures 7 and 8 show the histograms of the posterior marginal PDFs of the BMA weights for monthly rainfall totals of the individual ensemble members during the training period of Sylhet station for the pre-monsoon and monsoon season, respectively. All of the histograms exhibit gamma distribution, as discussed earlier. Therefore, we have high confidence in the weights applied to each of the individual models. The optimal values derived with the MCMC algorithm are indicated separately in each panel with an 'x' symbol. The optimal BMA weights for rainfall of six rainfall stations are presented in Figure 9. As noted previously, the BMA weights were calculated separately for the monthly rainfall during the pre-monsoon and monsoon seasons.

The BMA weight reflects the overall performance of the RCMs in capturing monthly rainfall for the study area. The RCMs showed better performance at one

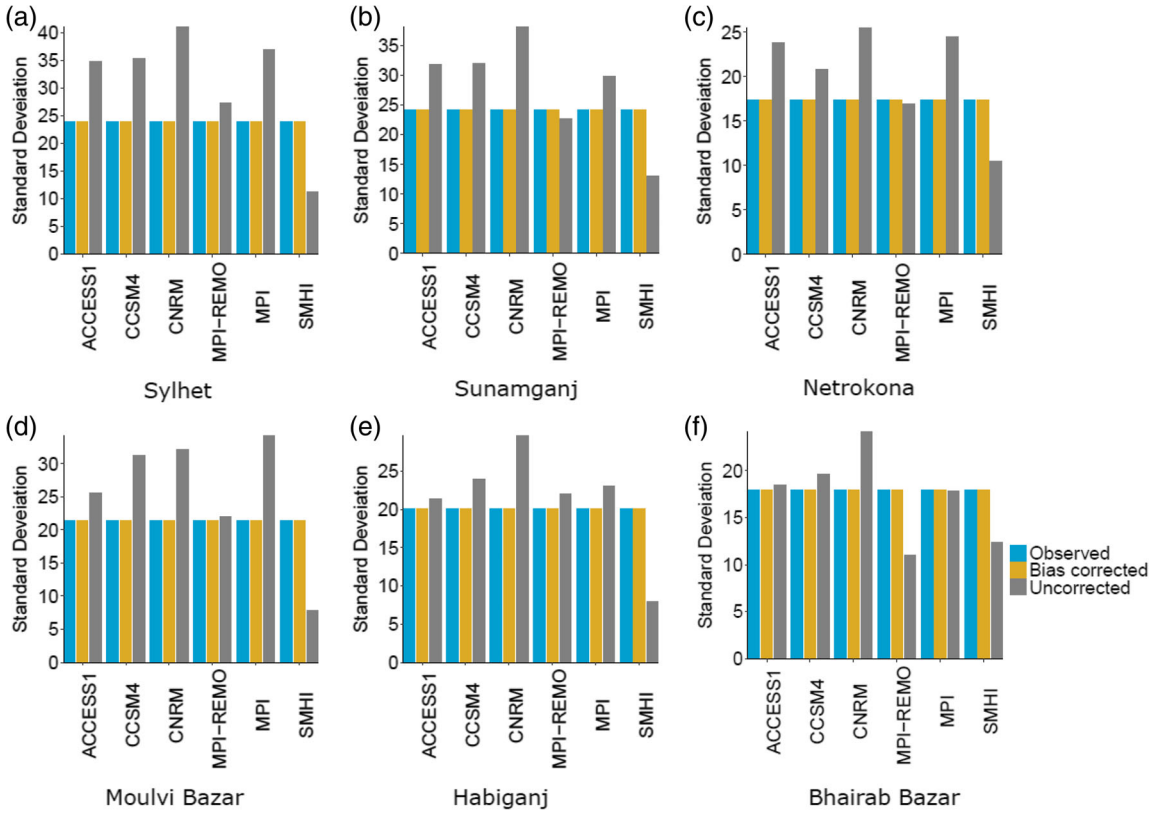

FIGURE 5 Comparison of the variability (i.e., standard deviation) between the bias-corrected and uncorrected simulations during the historical period (1976–2005) for pre-monsoon [Colour figure can be viewed at wileyonlinelibrary.com]

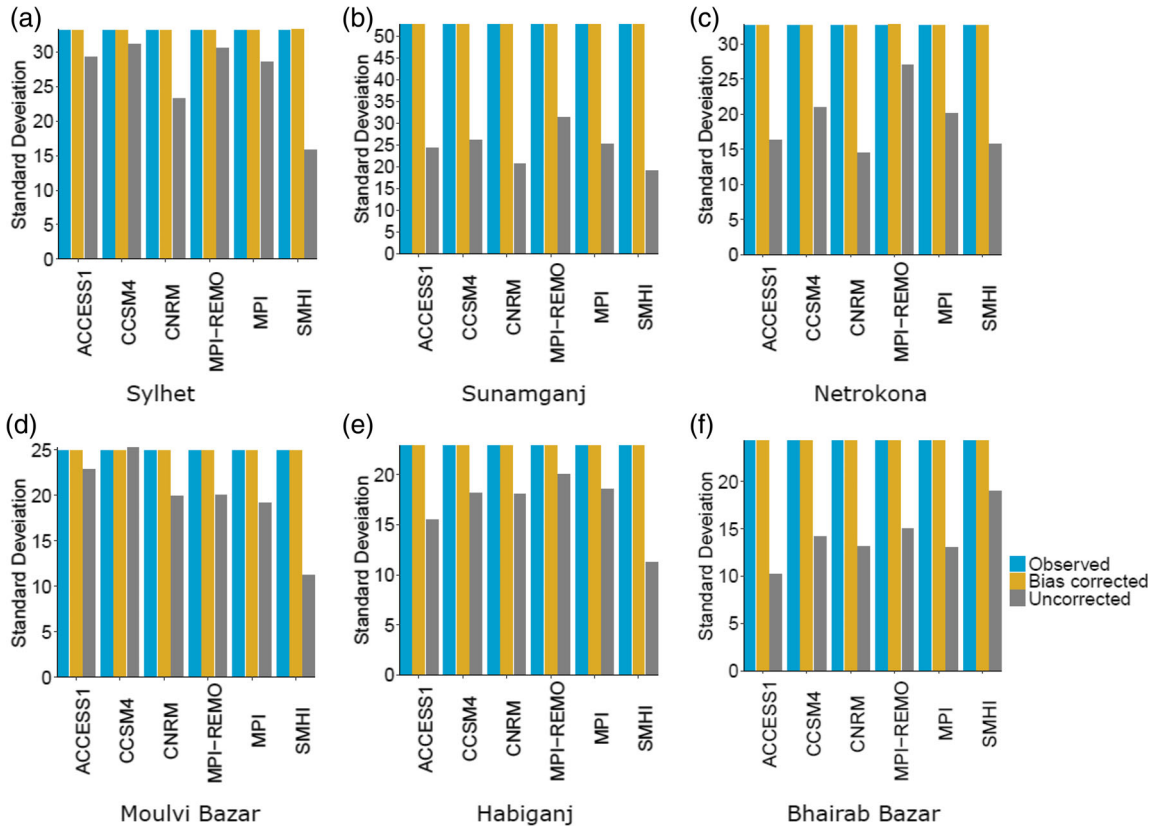

FIGURE 6 Comparison of the variability (i.e., standard deviation) between the bias-corrected and uncorrected simulations during the historical period (1976–2005) for monsoon [Colour figure can be viewed at wileyonlinelibrary.com]

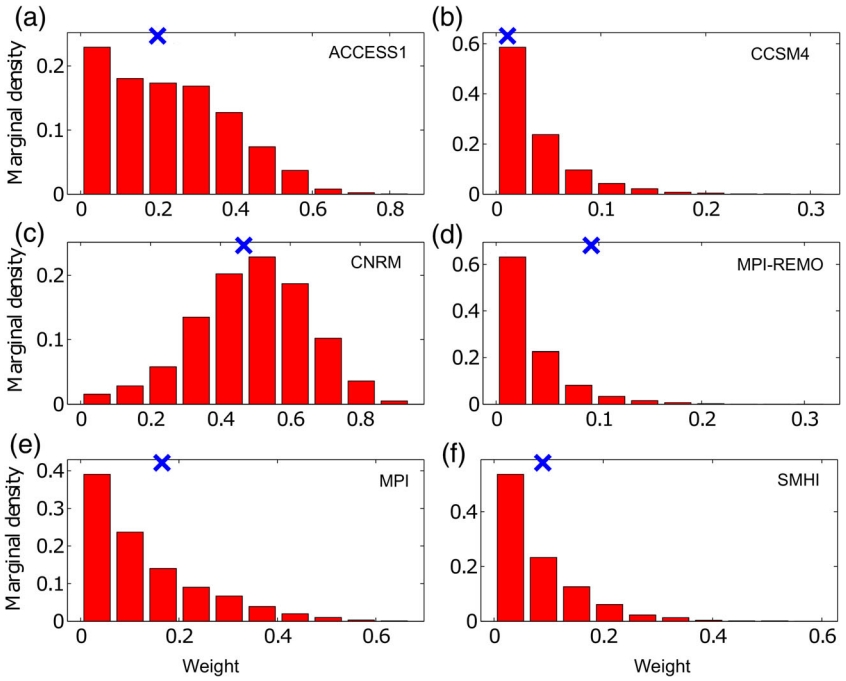

FIGURE 7 Marginal posterior PDFs of the DREAM-derived BMA weights of monthly rainfall totals for pre-monsoon Sylhet station. The MCMC-derived solution is indicated in each panel by the symbol 'X' [Colour figure can be viewed at wileyonlinelibrary.com]

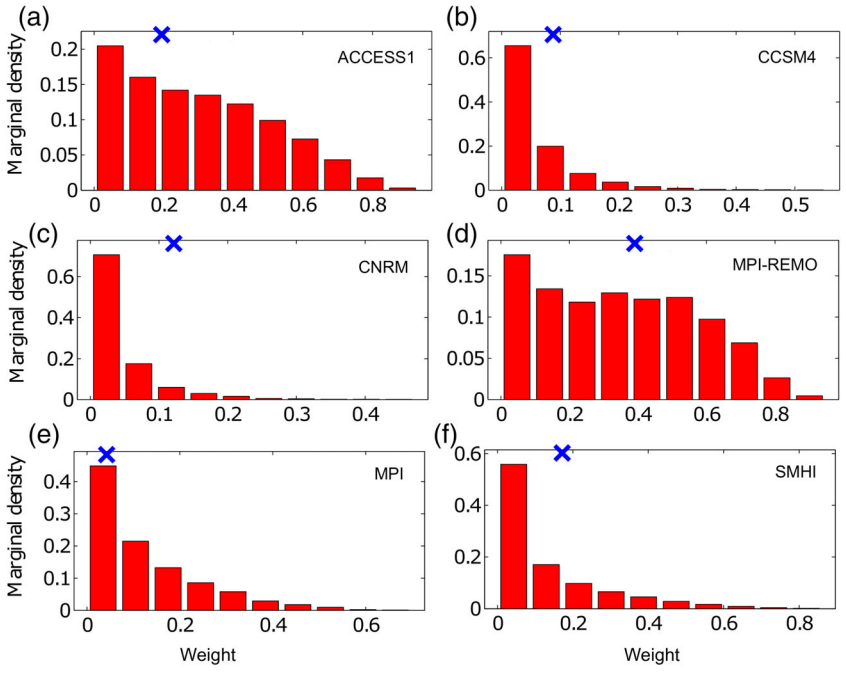

FIGURE 8 Marginal posterior PDFs of the DREAM-derived BMA weights of monthly rainfall totals for monsoon Sylhet station. The MCMC-derived solution is indicated in each panel by the symbol 'X' [Colour figure can be viewed at wileyonlinelibrary.com]

station and worse performance at another station. No particular RCM was consistent for capturing higher BMA weights for all stations (Figure 9). Similarly, the RCM performances varied in different seasons. This result infers that there is no single best or worst model in simulating rainfall variation over the region, in accordance with the concept of the multi-model approach.

We calculated the multi-model ensemble mean of rainfall using BMA weights and by the simple arithmetic ensemble mean (AEM). To evaluate the performance of BMA, we estimated the normalized root mean square error (NRMSE) (RMSE was normalized by the *SD* of observed data) for individual RCMs, BMA, and AEM (Table 5). It is noteworthy that the NRMSE of the commonly used AEM is always smaller than the corresponding statistic from each RCM for both seasons. This result is consistent with the general notion that the ensemble mean usually outperforms all or most of individual ensemble members (Raftery *et al.*, 2005). Relative to AEM, the NRMSE of the BMA is even smaller. The

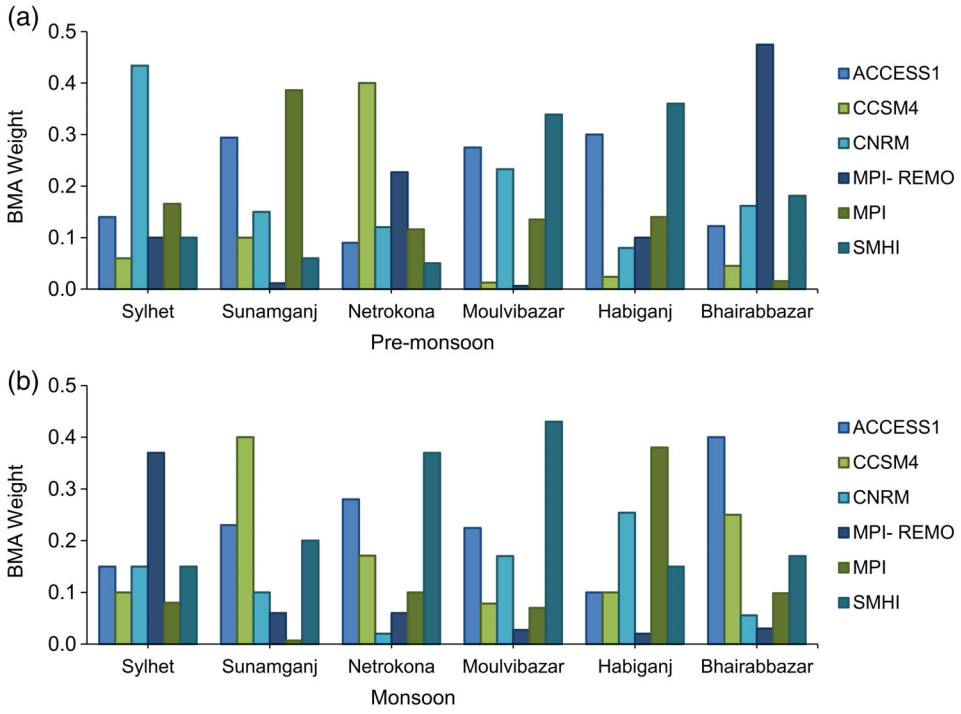

FIGURE 9 BMA weights of each individual RCM for monthly rainfall totals for different stations during historical period (1976–2005): (a) pre-monsoon and (b) monsoon [Colour figure can be viewed at wileyonlinelibrary.com]

TABLE 5 Normalized root mean square error (NRMSE) for seasonal rainfall of different RCMs, arithmetic ensemble mean (AEM), and BMA during historical period (1976–2005)

		ACCESS	CCSM4	CNRM	MPI-REMO	MPI	SMHI	AEM	BMA
Pre-monsoon	Sylhet	1.15	1.35	0.94	1.12	1.14	1.15	0.88	0.86
	Sunamganj	1.04	1.32	1.12	1.06	1.02	1.22	0.80	0.78
	Netrokona	1.17	1.01	1.10	0.96	1.13	1.22	0.75	0.72
	Moulvibazar	1.05	1.36	1.05	1.33	1.30	0.99	0.81	0.76
	Habiganj	1.14	1.58	1.20	1.34	1.40	1.02	0.82	0.78
	Bhiarabbazar	1.37	1.53	1.39	0.97	1.66	1.19	0.92	0.78
Monsoon	Sylhet	1.82	2.33	1.89	1.58	2.42	1.79	1.18	1.03
	Sunamganj	1.89	1.98	1.89	1.58	2.37	1.84	1.39	1.01
	Netrokona	2.25	1.95	1.95	1.72	2.34	1.76	1.22	1.07
	Moulvibazar	1.82	2.00	1.97	1.60	1.99	1.57	1.19	1.13
	Habiganj	2.01	2.32	2.48	1.76	1.94	1.85	1.65	1.24
	Bhiarabbazar	1.81	2.22	2.29	1.62	1.98	1.86	1.43	1.26

NRMSE of BMA is smaller than all participating RCMs for all stations and seasons. For all six stations, the average percentage of decrease in NRMSE from the AEM to BMA varies from 3% during the pre-monsoon to 22% during the monsoon season.

We assume that the BMA weights should reflect relative model skill in the multi-model ensemble approach. In other words, we anticipate that the RCMs with higher BMA weights should produce lower NRMSE. In fact, in some instances, the weights of the RCMs were not consistent with NRMSE. For example, the model MPI received the second-highest BMA weight at Sylhet station during the pre-monsoon season (Figure 9a) but ranked the third lowest NRMSE among the six RCMs (Table 5). The paired correlations could explain this inconsistent nature between individual simulations in the ensemble. Sometimes, the RCMs with the higher BMA weight may have a lesser correlation with the observed data and vice versa. This is due to a substantial amount of redundancy and results in de-weighing the best single simulation and overweighting of the worst single simulation. Other authors (Vrugt *et al.*, 2008; Woehling and Vrugt, 2008; Zhu *et al.*, 2013) also found this kind of inconsistency in their studies.

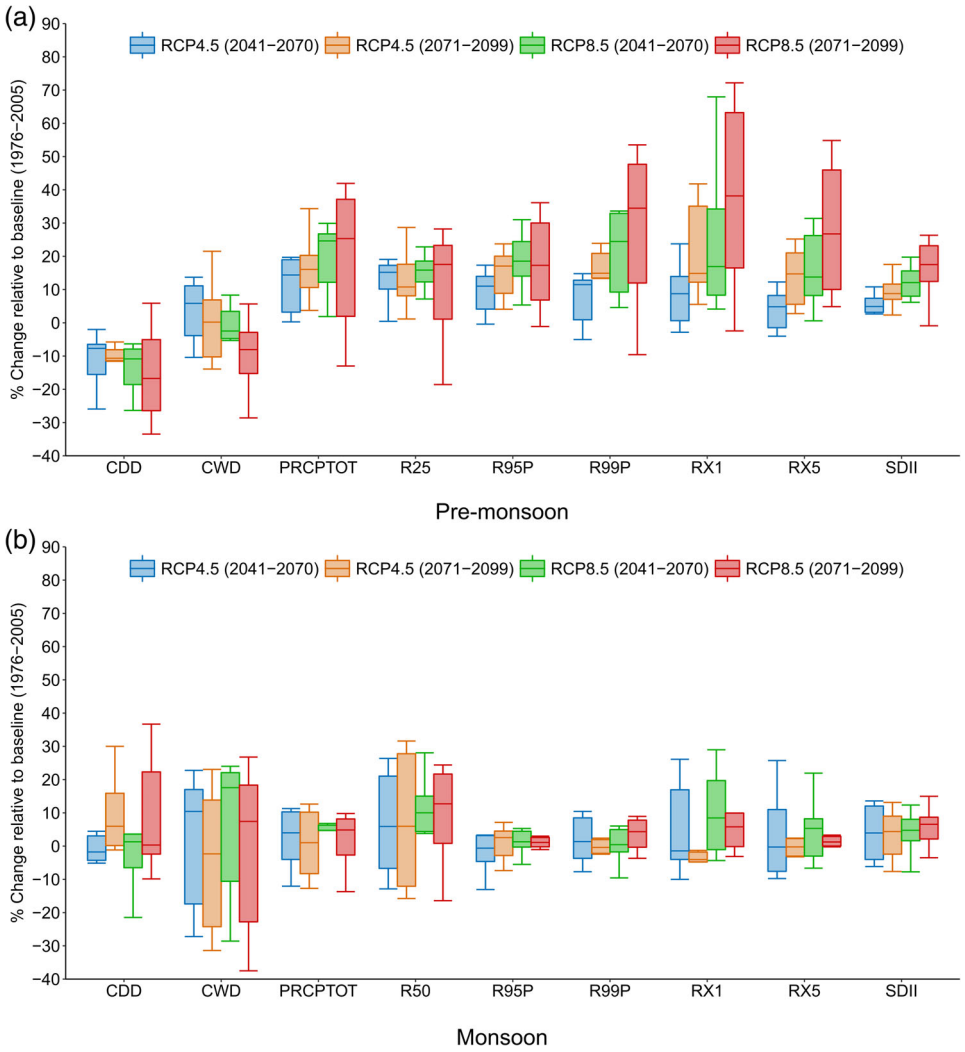

FIGURE 10 Box and whisker plots for changes in rainfall extremes at Sylhet station considering all RCMs for two future time slices (2041–2070 and 2071–2099) relative to the baseline period (1976–2005) under RCP4.5 and RCP8.5 scenarios: (a) pre-monsoon and (b) monsoon [Colour figure can be viewed at wileyonlinelibrary.com]

3.3 | Changes in future rainfall extremes

We estimate the changes in future rainfall extremes (listed in Table 2) for all RCMs (listed in Table 1) and for their ensemble mean generated by BMA weight. Figure 10 presents the variability of the mean changes in extreme indices with respect to the baseline for Sylhet station. During pre-monsoon, among all extreme indices, the variability of the relative changes is more significant for the one-day maximum rainfall (RX1) and less for the simple daily Intensity Index (SDII). This result implies that more uncertainty is associated with RX1 and less for SDII (Figure 10a). This result is not unexpected because the seasonal maximum daily rainfall is the single largest value in a season and the year to year variability of the value is large, while the rainfall intensity index is a quantity averaged over many days in a season. The uncertainty for all extremes indices is significant for the far future (2071–2099) and higher RCP (RCP8.5). Considering all RCMs, the mean relative changes are positive for all extreme indices except for consecutive dry days (CDDs) and consecutive wet days (CWDs) during the pre-monsoon at Sylhet station. Therefore, the CDDs become shorter over time. Similar to pre-monsoon, the uncertainty in relative changes is lesser for SDII during the monsoon (Figure 10b). Also note the large variability for CWD, CDD, and R50. The range of variability for changes in rainfall extremes is more significant during the pre-monsoon than the monsoon season. The variability of the extreme indices for other stations exhibit almost similar patterns to those of Sylhet (see Figures S3–S7).

To get an overview of the likely changes in extreme indices over the whole region, we looked at the range of the ensemble mean changes for all stations (Figure 11). In the pre-monsoon season (Figure 11a), the interquartile range of box plot is negative for CDD and positive for RX1, RX5, PRCPTOT, R25, SDII, R95P, and R99P in future time slices under the RCP4.5 and RCP8.5 over the study area. This phenomenon indicates an increasing level of changes for those indices with a positive range in the future. During the monsoon season (Figure 11b), the interquartile range of box plot is relatively smaller at

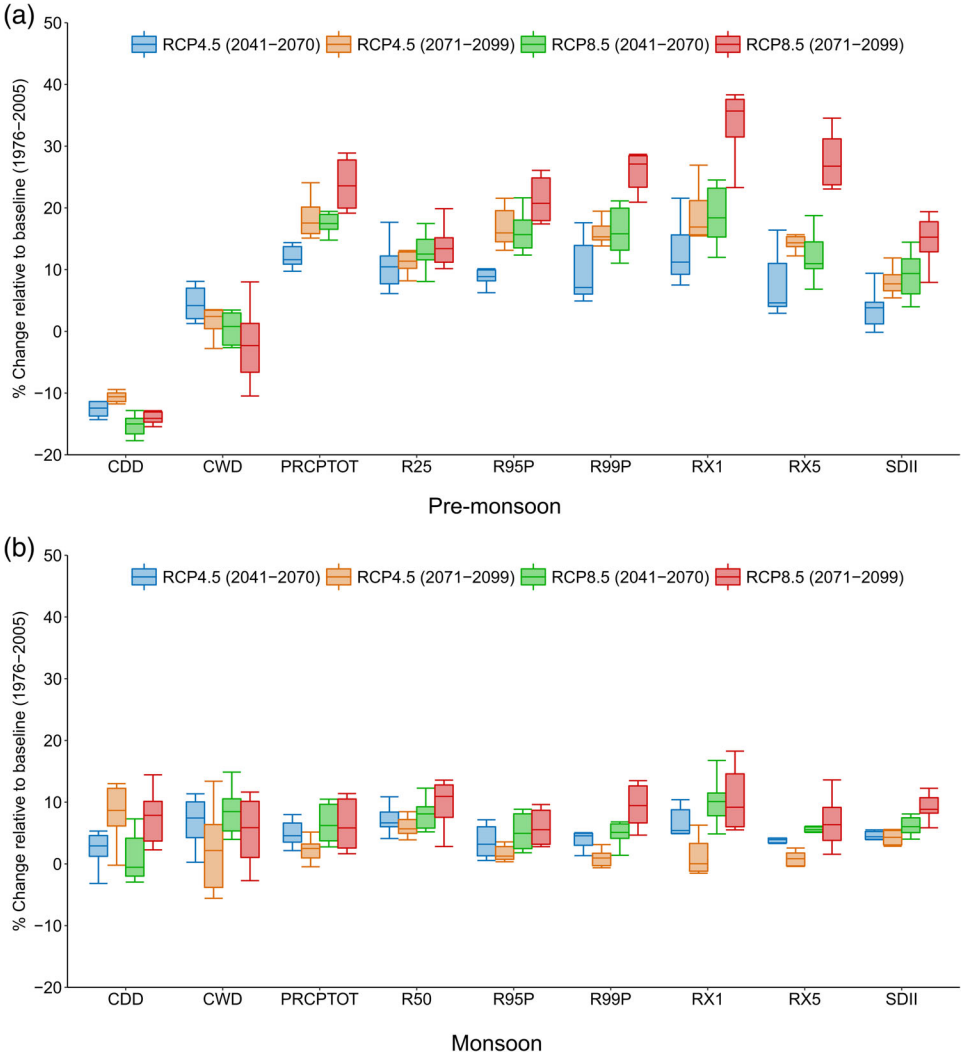

FIGURE 11 Box and whisker plots for changes of rainfall extremes over the study area considering all model ensemble mean derived by BMA for two future time slices (2041–2070 and 2071–2099) relative to the baseline period (1976–2005) under RCP4.5 and RCP8.5 scenarios: (a) pre-monsoon and (b) monsoon [Colour figure can be viewed at wileyonlinelibrary.com]

lower RCP (RCP4.5) during near future (2041–2070). However, it becomes more significant for higher RCP (RCP8.5) and the far future (2071–2099). The variability of all extreme indices is more significant during 2071–2099 under the RCP8.5 for both seasons than others. This result indicates that there is considerably more uncertainty associated with RCMs in projecting rainfall extremes as the RCP increases and time slice progresses from mid-century to the late century. Another important point is that the interquartile ranges of all extreme indices except CDD and CWD in both seasons are positive. This positive interquartile ranges of CDD and CWD means that all RCMs projected positive change. This result makes us more confident that these extreme indices are likely to increase in the future. On the other hand, the interquartile ranges of CDD in monsoon and CWD in both seasons vary between positive and negative values though their median values are positive. Therefore, we are less confident inferring that CDD and CWD are likely to increase in the future.

Average changes in rainfall extremes over the study area considering all stations multi-model ensemble mean derived by BMA are presented in Figure 12. All the extreme indices are projected to increase in the future except for a decrease in CDD and a slight decrease in CWD under RCP8.5 for 2071–2099 during the pre-monsoon season. During monsoon, all the extreme rainfall indices are likely to increase in the future under all scenarios (Figure 12b). However, the increasing rate of extreme indices is generally larger in pre-monsoon season than monsoon season. Moreover, all the extreme indices except CWD are likely to change significantly at the 95% confidence level during the pre-monsoon season (see Table 6). The average pre-monsoon rainfall of the study area is projected to increase by 12.93% for near future and 18.42% for far future under RCP4.5. Under the RCP8.5, it is projected to increase by 18.18% in the near future and 23.85% in far future (Figure 12a). During the monsoon, it is projected to increase by 4.96% in the near future and 2.27% in the far future under the RCP4.5, and

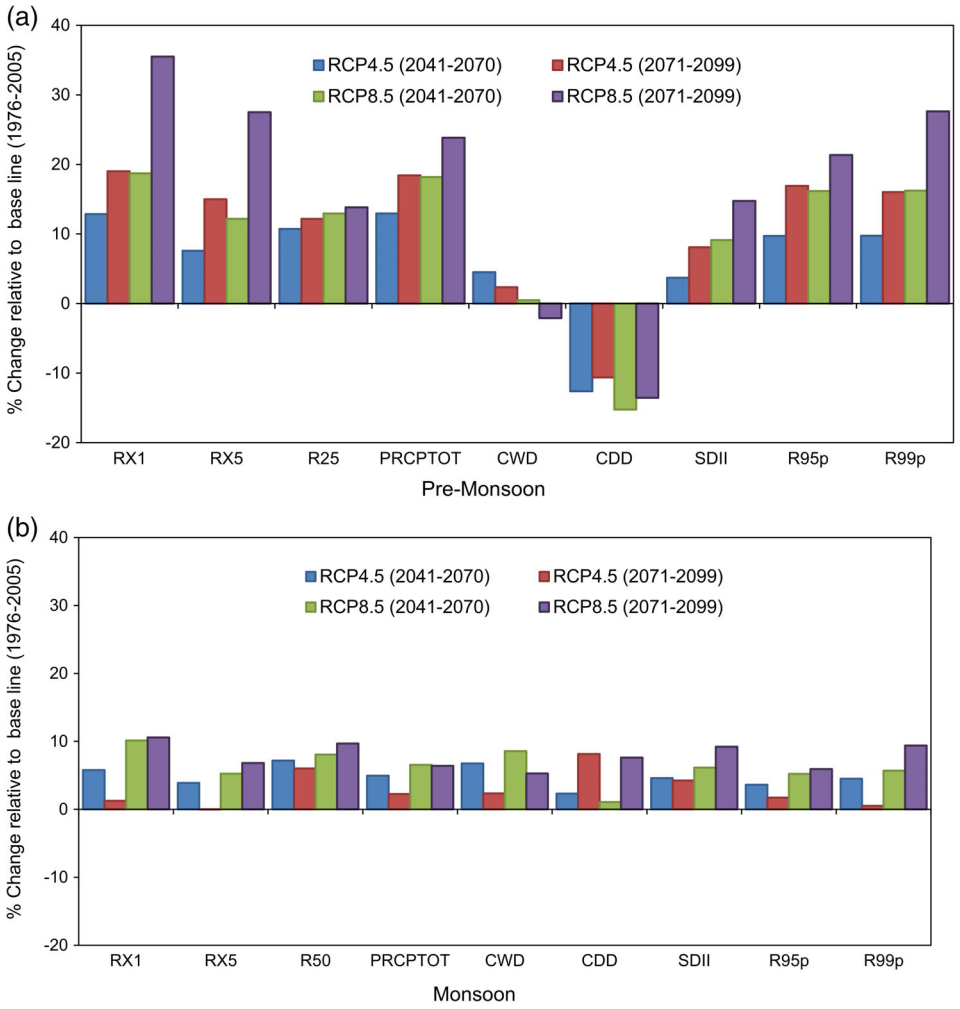

FIGURE 12 Average changes in rainfall extremes over the study area considering all model ensemble means derived by BMA for two future time slices (2041–2070 and 2071–2099) relative to the baseline period (1976–2005) under RCP4.5 and RCP8.5 scenarios: (a) pre-monsoon and (b) monsoon [Colour figure can be viewed at wileyonlinelibrary.com]

6.56% in the near future and 6.40% in far future under the RCP8.5. The results of this study are similar to studies (e.g., Akhter *et al*., 2017, Chen, 2013, Chen and Sun, 2013, Masood et al. 2015, Xu *et al*., 2019, Wu and Huang, 2016) conducted over several other countries in Asia. In those studies, they found that the extreme rainfall events over other parts of Asia are projected to significantly increase at the end of the 21st century. However, this study combined bias corrected multi-model ensemble means using BMA method to confirm such findings with a greater accuracy as it gives higher weight to the RCM with better predictive skill in the training period.

This increase in rainfall extremes in a warming world can be understood either by the dynamic process or the thermodynamic process (Vittal *et al*., 2016). In thermodynamic process, the intensity of extreme rainfall increases as temperature increases, which can be explained by the Clausius–Clapeyron (C-C) relationship. The atmospheric moisture-holding capacity is likely to increase with surface temperature according to the C-C equation (Panthou *et al*., 2014). Several studies (Vittal *et al*., 2016; Pfahl *et al*., 2017; Mukherjee *et al*., 2018) suggest that increased extreme rainfall over Indian is related to the dynamic process (changes in circulation pattern) rather than the thermodynamic process (e.g., changes in atmospheric moisture content). Moreover, the moisture availability is a more dominant factor than moisture-holding the capacity for changing extreme rainfall over this region (Vittal *et al*., 2016). This conclusion is further supported by Turner and Annamalai (2012) who argued that the increased rainfall is generally characterized by increased land-sea thermal contrast and atmospheric moisture content over the warmer Indian Ocean due to global warming. Several other studies (e.g., Cherchi *et al*., 2011; Asharaf and Ahrens, 2015; Sabeerali *et al*., 2015; Sharmila *et al*., 2015; Akhter *et al*., 2017) also argued that this increase in rainfall might be attributed to the increase of low-level (850 hPa) moisture content resulting from increased temperature due to global warming. For these reasons, due to climate change, the study area is expected to experience more frequent floods in the future in both the pre-monsoon and monsoon season. In particular, the intensity and magnitude of the flash flood in pre-monsoon are likely to increase more in the future as

TABLE 6 *p*-values of average changes of rainfall extremes over the study area considering all model ensemble mean in different RCP scenarios using Mann–Whitney *U* test. The extreme indices which changed significantly at 95% confidence level (*p*-value ≤ .05) are bold and underlined

	Index	RCP4.5 (2041–2070)	RCP4.5 (2071–2099)	RCP8.5 (2041–2070)	RCP8.5 (2071–2099)
Pre-monsoon	RX1	**0.013**	**0.000**	**0.000**	**0.000**
	RX5	0.100	**0.003**	**0.012**	**0.000**
	CDD	**0.003**	**0.020**	**0.001**	**0.002**
	CWD	0.234	0.581	0.919	0.323
	SDII	0.221	**0.038**	**0.011**	**0.000**
	PRCPTOT	**0.008**	**0.001**	**0.002**	**0.000**
	R99P	**0.023**	**0.001**	**0.001**	**0.000**
	R95P	**0.025**	**0.001**	**0.001**	**0.000**
	R25	**0.038**	**0.019**	**0.025**	**0.019**
Monsoon	RX1	0.149	0.963	**0.041**	**0.007**
	RX5	0.621	0.853	0.239	0.120
	CDD	0.756	0.090	0.797	0.075
	CWD	0.058	0.846	**0.034**	0.273
	SDII	0.193	0.233	**0.079**	**0.000**
	PRCPTOT	0.362	0.700	0.182	0.093
	R99P	0.286	0.877	0.145	**0.006**
	R95P	0.677	0.805	0.322	0.057
	R50	0.240	0.301	0.213	0.086

a result of the significant increase in the most extreme indices related to the occurrence of flash floods (e.g., PRCPTOT, RX1, SDII, R95p, and R99p) with a high decrease in CDD. This situation is projected to be more intense in the far future under the higher emission scenario.

4 | CONCLUSIONS

In this study, we analysed the impact of climate change on extreme rainfall in northeast Bangladesh using six RCMs over CORDEX South Asia domain under the RCP4.5 and RCP8.5. Generally, the RCMs are affected by biases inherited from the driving GCMs. We found that the RCMs overestimate the heavy rainfall events and underestimate low rainfall events during pre-monsoon season, and underestimate both during the monsoon season. Therefore, we applied the quantile mapping method to correct the bias associated with RCMs. We then used the BMA approach to generate the multi-model ensemble mean. The BMA mean is a weighted average related to each RCM's predictive skill. A closer look at each RCM showed that no single model was best or worst in simulating rainfall variations over northeast Bangladesh. However, the BMA produced more reliable results because NRMSE was lower than all six individual models and the arithmetic multi-model ensemble mean.

The results from the BMA indicate that the seasonal rainfall, together with other extreme indices, is likely to increase except for a decrease in CDD during pre-monsoon. However, the increasing rate of extreme indices is generally larger in the pre-monsoon season than monsoon season. The average pre-monsoon rainfall of the study area is projected to increase by 12.93% for near future and 18.42% for far future under RCP4.5. Under the RC8.5, it is projected to increase by 18.18% in the near future and 23.85% in far future (Figure 10a). During the monsoon, it is projected to increase by 4.96% in the near future and 2.27% in the far future under the RCP4.5. Under the RCP8.5, it is projected to increase 6.56% in the near future and 6.40% in the far future. Therefore, in the future, the study area is likely to experience more frequent floods in pre-monsoon and monsoon seasons under a warming climate. In particular, the intensity and magnitude of flash floods in the pre-monsoon are likely to increase more in the future as a result of the highly significant increase (*p*-value <.05) of all extreme indices related to the occurrence of the flash flood (e.g., PRCPTOT, RX1, SDII, R95p, and R99p). This situation is projected to be more intense in 2071–2099 than in 2041–2070.

These results indicate that the pre-monsoon season, in particular, may witness the most significant changes in rainfall in northeast Bangladesh. Seasonal rainfall together with other extreme indices is likely to increase, resulting in more frequent flash floods and putting the harvest of the Boro crop, as well as infrastructure and lives, at risk. This situation may intensify in the far future under a higher emission scenario.

ACKNOWLEDGEMENTS

This study has been funded by TRACKS (Transforming Climate Knowledge with and for Society: mobilizing knowledge on climate variability with communities in northeast Bangladesh) project sponsored by the Research Council of Norway. The climate projection data were provided from High End cLimatic Impacts and eXtremes (HELIX) project which received funding from the European Union Seventh Framework Programme FP7/2007-2013 under grant agreement no. 603864 (HELIX: High-End cLimate Impacts and eXtremes; http://www.helixclimate.eu).

ORCID

A. K. M. Saiful Islam https://orcid.org/0000-0002-2435-8280

Pao-Shin Chu https://orcid.org/0000-0002-8425-9559

REFERENCES

Ajami, N.K., Duan, Q. and Sorooshian, S. (2007) An integrated hydrologic Bayesian multi-model combination framework: confronting input, parameter, and model structural uncertainty in hydrologic prediction. *Water Resources Research*, 43(1), 1–19.

Alam, M.S., Quayum, M.A. and Islam, M.A. (2010) Crop production in the haor areas of Bangladesh: insights from farm level survey. *The Agriculturists*, 8(2), 88–97.

Akhter, J., Das, L. and Deb, A. (2017) CMIP5 ensemble-based spatial rainfall projection over homogeneous zones of India. *Climate Dynamics*, 49(5–6), 1885–1916.

Ashfaq, M., Bowling, L.C., Cherkauer, K., Pal, J.S. and Diffenbaugh, N.S. (2010) Influence of climate model biases and daily-scale temperature and precipitation events on hydrological impacts assessment: a case study of the United States. *Journal of Geophysical Research-Atmospheres*, 115(D14), 1–15.

Asharaf, S. and Ahrens, B. (2015) Indian summer monsoon rainfall processes in climate change scenarios. *Journal of Climate*, 28 (13), 5414–5429.

Bremer, S. (2017) Have we given up too much? On yielding climate representation to experts. *Futures*, 91, 72–75.

Chen, H. (2013) Projected change in extreme rainfall events in China by the end of the 21st century using CMIP5 models. *Chinese Science Bulletin, April 1, 2013*, 58(12), 1462–1472.

Chen, H. and Sun, J. (2013) Projected change in East Asian summer monsoon precipitation under RCP scenario. *Meteorology and Atmospheric Physics*, 121(1–2), 55–77.

Chen, J., Brissette, F.P. and Leconte, R. (2011) Uncertainty of downscaling method in quantifying the impact of climate change on hydrology. *Journal of Hydrology*, 401(3–4), 190–202.

Cherchi, A., Alessandri, A., Masina, S. and Navarra, A. (2011) Effects of increased CO2 levels on monsoons. *Climate Dynamics*, 37(1–2), 83–101.

Chu, P.S. and Zhao, X. (2011) Bayesian analysis for extreme climatic events: a review. *Atmospheric Research*, 102(3), 243–262.

Chu, P.S., Zhao, X., Karamperidou, C. and Zhang, H. (2016) Bayesian model averaging and its application to an El Niño index in CMIP5 models. In: *International Meetings on Statistical Climatology, 6–10 June*. Canmore: Canada.

Déqué, M., Somot, S., Sanchez-Gomez, E., Goodess, C.M., Jacob, D., Lenderink, G. and Christensen, O.B. (2012) The spread amongst ENSEMBLES regional scenarios: regional climate models, driving general circulation models and interannual variability. *Climate Dynamics*, 38(5–6), 951–964.

Dosio, A. and Paruolo, P. (2011) Bias correction of the ENSEMBLES high-resolution climate change projections for use by impact models: evaluation on the present climate. *Journal of Geophysical Research-Atmospheres*, 116(D16), 1–22.

Giorgi, F., Jones, C. and Asrar, G.R. (2009) Addressing climate information needs at the regional level: the CORDEX framework. *World Meteorological Organization Bulletin*, 58(3), 175.

Hasan, G.J., Alam, R.A., Islam, Q.N. and Hossain, M.S. (2012) Frequency structure of major rainfall events in the north-eastern part of Bangladesh. *Journal of Engineering Science and Technology*, 7(6), 690–700.

Hay, L.E. and Clark, M.P. (2003) Use of statistically and dynamically downscaled atmospheric model output for hydrologic simulations in three mountainous basins in the western United States. *Journal of Hydrology*, 82(1–4), 56–75.

Horton, P., Schaefli, B., Mezghani, A., Hingray, B. and Musy, A. (2006) Assessment of climate-change impacts on alpine discharge regimes with climate model uncertainty. *Hydrological Processes: An International Journal*, 20(10), 2091–2109.

Hoeting, J.A., Madigan, D., Raftery, A.E. and Volinsky, C.T. (1999) Bayesian model averaging: a tutorial. *Statistical Science*, 14(4), 382–401.

Islam, M.N. and Uyeda, H. (2007) Use of TRMM in determining the climatic characteristics of rainfall over Bangladesh. *Remote Sensing of Environment*, 108(3), 264–276.

Jacob, D., Petersen, J., Eggert, B., Alias, A., Christensen, O.B., Bouwer, L.M., Braun, A., Colette, A., Déqué, M., Georgievski, G. and Georgopoulou, E. (2014) EURO-CORDEX: new high-resolution climate change projections for European impact research. *Regional Environmental Change*, 14(2), 563–578.

Kay, A.L., Davies, H.N., Bell, V.A. and Jones, R.G. (2009) Comparison of uncertainty sources for climate change impacts: flood frequency in England. *Climatic Change*, 92(1–2), 41–63.

Kato, H., Nishizawa, K., Hirakuchi, H., Kadokura, S., Oshima, N. and Giorgi, F. (2001) Performance of RegCM2. 5/NCAR-CSM nested system for the simulation of climate change in East Asia caused by global warming. *Journal of the Meteorological Society of Japan. Ser. II*, 79(1), 99–121.

Katz, R.W. (1999) Extreme value theory for precipitation: sensitivity analysis for climate change. *Advances in Water Resources*, 23(2), 133–139.

Kim, K.B., Kwon, H.H. and Han, D. (2015) Bias correction methods for regional climate model simulations considering the distributional parametric uncertainty underlying the observations. *Journal of Hydrology*, 530, 568–579.

Kumar, K.R., Sahai, A.K., Kumar, K.K., Patwardhan, S.K., Mishra, P.K., Revadekar, J.V., Kamala, K. and Pant, G.B. (2006)

High-resolution climate change scenarios for India for the 21st century. *Current Science*, 90(3), 334–345.

Leander, R. and Buishand, T.A. (2007) Resampling of regional climate model output for the simulation of extreme river flows. *Journal of Hydrology*, 332(3–4), 487–496.

Leander, R., Buishand, T.A., van den Hurk, B.J. and de Wit, M.J. (2008) Estimated changes in flood quantiles of the river Meuse from resampling of regional climate model output. *Journal of Hydrology*, 351(3–4), 331–343.

Lehner, B., Döll, P., Alcamo, J., Henrichs, T. and Kaspar, F. (2007) Estimating the impact of global change on flood and drought risks in Europe: a continental, integrated analysis. *Climatic Change*, 75(3), 273–299.

Mahanta, R., Sarma, D. and Choudhury, A. (2013) Heavy rainfall occurrences in Northeast India. *International Journal of Climatology*, 33(6), 1456–1469.

Masood, M., Yeh, P. F., Hanasaki, N. and Takeuchi, K. (2015) Model study of the impacts of future climate change on the hydrology of Ganges–Brahmaputra–Meghna basin. *Hydrology and Earth System Sciences*, 19(2), 747–770.

Masood, M. and Takeuchi, K. (2016) Climate change impacts and its implications on future water resource management in the Meghna Basin. *Futures*, 78, 1–18.

Mearns, L.O., Arritt, R., Biner, S., Bukovsky, M.S., McGinnis, S., Sain, S., Caya, D., Correia, J., Jr., Flory, D., Gutowski, W. and Takle, E.S. (2012) The north American regional climate change assessment program: overview of phase I results. *Bulletin of the American Meteorological Society*, 93(9), 1337–1362.

Maraun, D., Wetterhall, F., Ireson, A.M., Chandler, R.E., Kendon, E.J., Widmann, M., Brienen, S., Rust, H.W., Sauter, T., Themeßl, M. and Venema, V.K. (2010) Precipitation downscaling under climate change: recent developments to bridge the gap between dynamical models and the end user. *Reviews of Geophysics*, 48(3), 1–34.

Mukherjee, S., Aadhar, S., Stone, D. and Mishra, V. (2018) Increase in extreme precipitation events under anthropogenic warming in India. *Weather and Climate Extremes*, 20(2018), 45–53.

Neuman, S.P. (2003) Maximum likelihood Bayesian averaging of uncertain model predictions. *Stochastic Environmental Research and Risk Assessment*, 17(5), 291–305.

Nowreen, S., Murshed, S.B., Islam, A.S., Bhaskaran, B. and Hasan, M.A. (2015) Changes of rainfall extremes around the haor basin areas of Bangladesh using multi-member ensemble RCM. *Theoretical and Applied Climatology*, 119(1–2), 363–377.

Ohsawa, T., Ueda, H., Hayashi, T., Watanabe, A. and Matsumoto, J. (2001) Diurnal variations of convective activity and rainfall in tropical Asia. *Journal of the Meteorological Society of Japan. Ser. II*, 79(1B), 333–352.

Panthou, G., Mailhot, A., Laurence, E. and Talbot, G. (2014) Relationship between surface temperature and extreme rainfalls: a multi-time-scale and event-based analysis. *Journal of Hydrometeorology*, 15(5), 1999–2011.

Pfahl, S., O'Gorman, P.A. and Fischer, E.M. (2017) Understanding the regional pattern of projected future changes in extreme precipitation. *Nature Climate Change*, 7(6), 423.

Piani, C., Haerter, J.O. and Coppola, E. (2010) Statistical bias correction for daily precipitation in regional climate models over Europe. *Theoretical and Applied Climatology*, 99(1–2), 187–192.

Pierce, D.W., Barnett, T.P., Santer, B.D. and Gleckler, P.J. (2009) Selecting global climate models for regional climate change studies. *Proceedings of the National Academy of Sciences*, 106 (21), 8441–8446.

Rafiuddin, M., Uyeda, H. and Islam, M.N. (2010) Characteristics of monsoon precipitation systems in and around Bangladesh. *International Journal of Climatology*, 30(7), 1042–1055.

Raftery, A.E., Madigan, D. and Hoeting, J.A. (1997) Bayesian model averaging for linear regression models. *Journal of the American Statistical Association*, 92(437), 179–191.

Raftery, A.E., Gneiting, T., Balabdaoui, F. and Polakowski, M. (2005) Using Bayesian model averaging to calibrate forecast ensembles. *Monthly Weather Review*, 133(5), 1155–1174.

Räisänen, J. and Räty, O. (2013) Projections of daily mean temperature variability in the future: cross-validation tests with ENSEMBLES regional climate simulations. *Climate Dynamics*, 41(5–6), 1553–1568.

Revadekar, J.V., Patwardhan, S.K. and Rupa Kumar, K. (2011) Characteristic features of precipitation extremes over India in the warming scenarios. *Advances in Meteorology*, 2011, 1–11.

Rauscher, S.A., Coppola, E., Piani, C. and Giorgi, F. (2010) Resolution effects on regional climate model simulations of seasonal precipitation over Europe. *Climate Dynamic*, 35(4), 685–711.

Sato, T. (2013) Mechanism of orographic precipitation around the Meghalaya plateau associated with intraseasonal oscillation and the diurnal cycle. *Monthly Weather Review*, 141(7), 2451–2466.

Sabeerali, C.T., Rao, S.A., Dhakate, A.R., Salunke, K. and Goswami, B.N. (2015) Why ensemble mean projection of south Asian monsoon rainfall by CMIP5 models is not reliable? *Climate Dynamics*, 45(1–2), 161–174.

Schmidli, J. and Frei, C. (2005) Trends of heavy precipitation and wet and dry spells in Switzerland during the 20th century. *International Journal of Climatology*, 25(6), 753–771.

Sennikovs, J. and Bethers, U. (2009) Statistical downscaling method of regional climate model results for hydrological modelling (009). In: *In Proceedings 18th World IMACS/MODSIM Congress*. Cairns, Australia: MSSANZ.

Sharmila, S., Joseph, S., Sahai, A.K., Abhilash, S. and Chattopadhyay, R. (2015) Future projection of Indian summer monsoon variability underclimate change scenario: an assessment from CMIP5 climate models. *Global and Planetary Change*, 124, 62–78.

Stiller-Reeve, M.A., Syed, M.A., Spengler, T., Spinney, J.A. and Hossain, R. (2015) Complementing scientific monsoon definitions with social perception in Bangladesh. *Bulletin of the American Meteorological Society*, 96(1), 49–57.

Teutschbein, C. and Seibert, J. (2010) Regional climate models for hydrological impact studies at the catchment scale: a review of recent modeling strategies. *Geography Compass*, 4(7), 834–860.

Teutschbein, C. and Seibert, J. (2012) Bias correction of regional climate model simulations for hydrological climate-change impact studies: review and evaluation of different methods. *Journal of Hydrology*, 456, 12–29.

Themeßl, M.J., Gobiet, A. and Heinrich, G. (2012) Empirical-statistical downscaling and error correction of regional climate models and its impact on the climate change signal. *Climatic Change*, 112(2), 449–468.

Turco, M., Quintana-Seguí, P., Llasat, M.C., Herrera, S. and Gutiérrez, J.M. (2011) Testing MOS precipitation downscaling

for ENSEMBLES regional climate models over Spain. *Journal of Geophysical Research-Atmospheres*, 116(D18), 1–14.

Turner, A.G. and Annamalai, H. (2012) Climate change and the South Asian summer monsoon. *Nature Climate Change*, 2 (8), 587.

Villani, V., Rianna, G., Mercogliano, P. and Zollo, A.L. (2015) Statistical approaches versus weather generator to downscale RCM outputs to slope scale for stability assessment: a comparison of performances. *Electronic Journal Geotechnical Engineering*, 20(4), 1495–1515.

Vittal, H., Ghosh, S., Karmakar, S., Pathak, A. and Murtugudde, R. (2016) Lack of dependence of Indian summer monsoon rainfall extremes on temperature: an observational evidence. *Scientific Reports*, 6, 31039.

Vrugt, J.A. and Robinson, B.A. (2007) Treatment of uncertainty using ensemble methods: comparison of sequential data assimilation and Bayesian model averaging. *Water Resources Research*, 43(1), 1–15.

Vrugt, J.A., Diks, C.G. and Clark, M.P. (2008) Ensemble Bayesian model averaging using Markov chain Monte Carlo sampling. *Environmental Fluid Mechanics*, 8(5–6), 579–595.

Vrugt, J.A. (2015) Multi-criteria optimization using the AMALGAM software package: theory, concepts, and MATLAB implementation. *Manual, Version*, 1, 1–53.

Vrugt, J.A. (2016) Markov chain Monte Carlo simulation using the DREAM software package: theory, concepts, and MATLAB implementation. *Environmental Modelling and Software*, 75, 273–316.

Winkler, J.A., Guentchev, G.S., Tan, P.N., Zhong, S., Liszewska, M., Abraham, Z., Niedźwiedź, T. and Ustrnul, Z. (2011) Climate scenario development and applications for local/regional climate change impact assessments: an overview for the non-climate scientist: part I: scenario development using downscaling methods. *Geography Compass*, 301–328, 275–300.

Woehling, T. and Vrugt, J.A. (2008) Combining multi objective optimization and Bayesian model averaging to calibrate forecast ensembles of soil hydraulic models. *Water Resources Research*, 44(12), 1–18.

Wu, C.H., Huang, G.R. and Yu, H.J. (2015) Prediction of extreme floods based on CMIP5 climate models: a case study in the Beijiang River basin, South China. *Hydrology and Earth System Sciences*, 19, 1385–1399.

Wu, C. and Huang, G. (2016) Projection of climate extremes in the Zhujiang River basin using a regional climate model. *International Journal of Climatology*, 36(3), 1184–1196.

Xu, K., Xu, B., Ju, J., Wu, C., Dai, H. and Hu, B.X. (2019) Projection and uncertainty of precipitation extremes in the CMIP5 multi-model ensembles over nine major basins in China. *Atmospheric Research*, 226, 122–137.

Zhang, X., Xiong, Z., Zhang, X., Shi, Y., Liu, J., Shao, Q. and Yan, X. (2016) Using multi-model ensembles to improve the simulated effects of land use/cover change on temperature: a case study over Northeast China. *Climate Dynamics*, 46(3–4), 765–778.

Zhang, H., Chu, P.S., He, L. and Unger, D. (2019) Improving the CPC's ENSO forecasts using Bayesian model averaging. *Climate Dynamics*, 53, 3373–3385.

Zhu, R., Zheng, H., Wang, E. and Zhao, W. (2013). *Multi-model ensemble simulation of flood events using Bayesian model averaging*. In MODSIM2013, 20th International Congress on Modelling and Simulation, Modelling and Simulation Society of Australia and New Zealand, pp. 455–461.

Zorita, E. and Von Storch, H. (1999) The analog method as a simple statistical downscaling technique: comparison with more complicated methods. *Journal of Climate*, 12(8), 2474–2489.

SUPPORTING INFORMATION

Additional supporting information may be found online in the Supporting Information section at the end of this article.

How to cite this article: Basher A, Islam A. K. M. Saiful, Stiller-Reeve MA, Chu P-S. Changes in future rainfall extremes over Northeast Bangladesh: A Bayesian model averaging approach. *Int J Climatol*. 2020;40:3232–3249. https://doi.org/10.1002/joc.6394